Manipulation of resonances in an open three-terminal interferometer with an embedded quantum dot

Yong S. Joe and Eric R. Hedin
Center for Computational Nanoscience, Department of Physics and Astronomy, Ball State University, Muncie, Indiana 47306, USA

Arkady M. Satanin
Institute for Physics of Microstructures, RAS, GSP-105, Nizhny Novgorod, 603950 Russia

(Received 12 April 2007; published 17 August 2007)

A three-terminal Aharonov-Bohm ring with a quantum dot embedded in one arm is investigated using the exactly solvable formalism of the tight-binding model. We show that by tuning the degree of coupling to the third terminal, the zero of the Fano resonance in the transmission moves off the real-energy axis and the phase jump of π at the resonance diminishes and softens. This behavior is illustrated with a simple model involving the zero and pole of the Fano resonance. The manifestation of the Fano resonance on the conductance, due to the unique interplay between the magnetic flux through the ring and coupling to the third terminal, is discussed.

DOI: 10.1103/PhysRevB.76.085419 PACS number(s): 73.21.La, 73.23.Ad, 73.63.Kv, 85.35.Ds

Electron transmission through quantum dots (QD) and Aharonov-Bohm (AB) rings has shown a rich resonance structure, which includes Fano resonances[1] when the QD is embedded in one arm of the AB ring. The Fano resonance is a manifestation of interference between the localized quasibound states of the QD in one arm and the continuum states in the other arm, characterized by both complete transmission and complete reflection. This characteristic of resonance structure (a zero-pole pair) can be controlled by changing the confinement parameters of the QD. Transmission through a QD embedded in an AB ring remains phase coherent, as indicated by the visibility of the AB oscillations.[2] The intrinsic phase of the QD is significant in its relation to the AB oscillations when the QD is embedded in the AB ring, and it has experimentally been seen to exhibit interesting phase jumps of π in a *two-terminal* system when the conductance of the AB ring reaches a peak.[3,4] Aharony *et al.* show that this "phase rigidity" can be broken in physical AB rings with several electron paths around the ring. In this case, each resonance on the QD couples to a different wave function on the ring (associated with a different enclosed flux), leading to different periodicities of the AB oscillations.[5]

Theoretical analysis of these systems[6] has provided some explanation for the phase behavior that has been observed in experiments. In a two-terminal device (single-path device), the Onsager relations[7] of time-reversal symmetry and current conservation (unitarity) constrain the transmission phase to values of 0 or π. However, if the two-terminal AB ring is "opened" by allowing current to flow out through additional terminals, the unitarity condition is broken and it becomes possible to extract meaningful phase information about the QD.[8–10] Experiments with open rings demonstrate a gradual, rather than abrupt, phase change across the transmission resonances, as measured by the phase of the AB oscillations.[11] In particular, Schuster *et al.* produced a four-terminal interferometer in an AlGaAs/GaAs heterostructure which showed smooth phase transitions.[3] Other mechanisms, which have been postulated to contribute to the disruption of unitarity, include QD interlevel thermal excitation and inelastic electron-phonon interactions.[12]

In this article we analyze a three-terminal interferometer with an embedded QD in one arm of the AB ring. By employing the exactly solvable formalism of the tight-binding model, the electron transmission (conductance) through the ring and the transmission phase are studied by modulating the coupling, V_D, of the QD to a third output terminal. As V_D is increased from zero (creating an open ring), the zero of the Fano resonance produced by the QD and the AB ring leaves the real-energy axis and the abrupt phase jump of π is seen to soften. Other recent research on the mesoscopic Fano effect shows that for the case of imperfect coupling between the arms of the AB interferometer, the transmission consists of mixed modes which inhibit the complete destructive interference characteristic of the Fano resonance zero.[13] In the research presented here, however, we focus on the case of complete coupling between the AB arms. A simple analytical model of the Fano resonances shows naturally how the phase transition across the resonance peak softens in the case where the transmission zero is no longer real, but complex. In contrast, the transmission to the third output terminal shows a simple Breit-Wigner (BW) resonance with the corresponding transmission phase near the BW resonance changing by π progressively more smoothly for $V_D > 0$. We also show the magnetic flux dependence of the transmission (conductance) and the resistance for an open ring with a fixed coupling V_D. Experiments have shown a slight flux dependence of the transmission resonances and the phase of the AB oscillations.[5,14] However, this effect is insignificant if the area of the QD is small compared to the ring area (as assumed here), or for the case of weak fields.[15] Finally, we emphasize that for values of magnetic flux which position the Fano zero in the positive complex-energy half plane, the zero in the transmission can be returned to the real-energy axis by increasing V_D (effecting complete blockage of transmission into either terminal). This shows the unique control over resonance features offered in an open ring by the combination of phase effects arising from both magnetic flux and coupling to a third terminal.

The general structure studied in our calculations is a three-terminal AB ring with magnetic flux through the ring

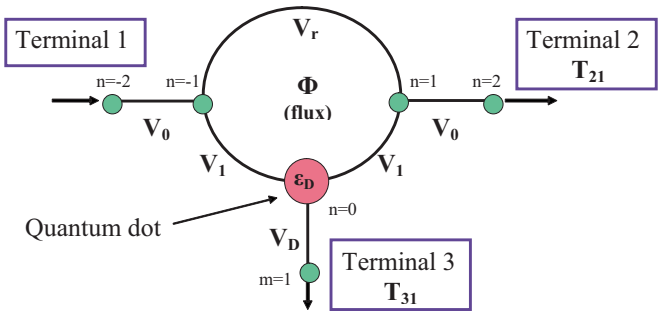

FIG. 1. (Color online) Schematic of the three-terminal interferometer with a QD embedded in one of the arms. In addition to the magnetic flux Φ threading the AB ring, the relevant coupling parameters between sites are defined: the confinement V_1 of the QD, coupling V_D to the third terminal, and coupling V_r through the reference arm of the ring.

and an embedded QD, sketched schematically in Fig. 1 where relevant parameters are defined. By discretizing the system spatially with lattice constant a, and denoting the wave function on site n by ψ_n, the Schrödinger equation in the tight-binding approximation can be written as $-\Sigma V_{n,m}\psi_m+\varepsilon_n\psi_n=E\psi_n$. Here, the sum runs over the nearest neighbors of n, E is the electron energy, and ε_n is the site energy. (In our calculations, the site energies ε_n are set to zero for all sites except for the QD at $n=0$ which has site energy ε_D.) The parameters $V_{n,m}$ are overlap integrals (or coupling parameters) involving the overlap of the single site, atomiclike wave functions from sites m and n with the single-site potential of site n. In the homogeneous leads, the coupling parameters are all set to $V_0=1.0$, which we use throughout the discussion as a unit of energy. In the presence of the magnetic flux Φ, a phase difference between the path through the QD and the path through the reference arm is produced.[16] Therefore, we choose a gauge in which the coupling parameter for each segment of the lower arm is modified as $V_1 \rightarrow V_1 e^{\pm i\varphi}$, and the reference arm coupling parameter becomes $V_r e^{\pm 2i\varphi}$ ("+" for counterclockwise transits around the ring and "−" for clockwise transits). The phase φ is related to the magnetic flux Φ by $2\varphi=\pi\Phi/\Phi_0$, where $\Phi_0=h/e$ is the elementary flux quantum.

Let us consider an incoming wave function only from terminal 1, with transmitted waves through the ring into the other terminals:

$$\psi_n = e^{in\theta} + r_{11}e^{-in\theta}, \quad n \leqslant -1,$$

$$\psi_n = t_{21}e^{in\theta}, \quad n \geqslant 1,$$

$$\psi_m = t_{31}e^{im\theta}, \quad m \geqslant 1, \tag{1}$$

with $\theta=ka$. Here, k is the wave vector that is connected with the energy by the dispersion relation for the Bloch states, $E=-2V_0\cos ka$; t_{21} and t_{31} are the transmission amplitudes from terminal 1 into terminal 2 and 3, respectively; and r_{11} is the reflection amplitude back to terminal 1. Applying the Schrödinger equation to the three sites around the AB ring and also to site $m=1$ of the third terminal, we obtain the following matrix equation for the complex transmission amplitudes:

$$\begin{pmatrix} V_0 & -V_r e^{-i(2\varphi-\theta)} & -V_1 V_0 e^{i\varphi}/V_D \\ -V_r e^{i(2\varphi+\theta)} & V_0 & -V_1 V_0 e^{-i\varphi}/V_D \\ -V_1 e^{-i(\varphi-\theta)} & -V_1 e^{i(\varphi+\theta)} & -(V_D e^{i\theta}+(E-\varepsilon_D)V_0/V_D) \end{pmatrix} \times \begin{pmatrix} r_{11} \\ t_{21} \\ t_{31} \end{pmatrix} = \begin{pmatrix} -V_0 \\ V_r e^{i(2\varphi-\theta)} \\ V_1 e^{-i(\varphi+\theta)} \end{pmatrix}. \tag{2}$$

Inverting the matrix on the left side of Eq. (2), we can find the unknown reflection and transmission amplitudes: r_{11}, t_{21}, and t_{31}. In the same way we can find the other elements of the scattering matrix: r_{22}, t_{12}, t_{32} and r_{33}, t_{13}, t_{23} when incoming waves are chosen from terminals 2 and 3, respectively. The transmission amplitudes for an electron from terminal (channel) j into terminal (channel) i may be written in the form[17]

$$t_{ij}(\Phi) = \frac{N_{ij}(\Phi)}{D(\Phi)}, \tag{3}$$

where we have

$$N_{21}(\Phi) = 2iV_0 \sin\theta e^{2i\varphi}[V_r(V_0(E-\varepsilon_D)+e^{i\theta}V_D^2) - e^{-4i\varphi}V_0V_1^2], \tag{4}$$

$$N_{31}(\Phi) = -2iV_0V_1V_D \sin\theta e^{-i\varphi}[V_0 + e^{i(4\varphi+\theta)}V_r], \tag{5}$$

$$D(\Phi) = e^{i\theta}V_0^2(2V_1^2+V_D^2) - e^{3i\theta}V_r^2V_D^2 + V_0(V_0^2 - e^{2i\theta}V_r^2)(E - \varepsilon_D) + 2e^{2i\theta}V_0V_rV_1^2\cos(4\varphi), \tag{6}$$

with symmetry conditions

$$D(\Phi) = D(-\Phi), \quad N_{ij}(\Phi) = N_{ji}(-\Phi), \quad N_{13}(\Phi) = N_{23}(\Phi). \tag{7}$$

Thus, we have all the transmission coefficients $T_{ij}(\Phi) = |t_{ji}(\Phi)|^2$, which obey the property

$$T_{ij}(\Phi) = T_{ji}(-\Phi). \tag{8}$$

In order to find the nonlocal conductance of the open ring, we use the Buttiker equations:[18]

$$I_i = \frac{2e}{h}\left[(1-R_{ii})\mu_i - \sum_{j\neq i} T_{ij}\mu_j\right] \quad (i,j=1,2,3), \tag{9}$$

where $R_{ij}(\Phi)=|r_{ji}(\Phi)|^2$ are the reflection coefficients (which may be eliminated from the set of equations by using current conservation: $1-R_{ii}=\Sigma_{j\neq i}T_{ij}$), and μ_i are the chemical potentials of the reservoirs (terminals). The factor of 2 in Eq. (9) stems from the identical contribution of both electron spin states. Here, it is noteworthy that we consider a typical situation in which two terminals (1 and 2) are used for injection of current and measurements of the conductance $G_{12,12}$ (see Büttiker's notations in Ref. 18), whereas the potential drop (which is characterized by the resistance $R_{12,13}$) is measured only between terminals 1 and 3. For our purpose, we set the current between terminals 1 and 2 as $I \equiv I_1 = -I_2$.

Thus, terminal 3 represents an ideal probe that draws no net current ($I_3=0$). Solving the set of Eq. (9), we find the coefficient

$$G_{12,12} = \frac{2e^2}{h}\left(T_{21} + \frac{T_{23}T_{31}}{T_{31}+T_{32}}\right) \tag{10}$$

between the current I and the bias $U_{12}=(\mu_1-\mu_2)/e$. The potential drop U_{13} between the terminals 1 and 3 is defined by the resistance $R_{12,13}$, $U_{13}=R_{12,13}I$, where

$$R_{12,13} = \frac{h}{2e^2}\left(\frac{T_{32}}{T_{21}T_{31}+T_{23}T_{31}+T_{32}T_{21}}\right). \tag{11}$$

Below, we present results for the following parameters of the system: $V_1=0.3$ (QD confinement), $V_r=0.3$ (the coupling through the reference arm of the AB ring), and $\varepsilon_D=0$ (the site energy of the QD which positions the resonance in the center of the allowed energy band).

Now, we study the effect of coupling to the third output terminal on the transmission $T_{21}=|t_{21}|^2$ through the AB ring in the absence of the magnetic flux. Here, the transmission amplitude t_{21} can be calculated from Eq. (3) as

$$t_{21} = \frac{2i\sin\theta[V_1^2 - e^{4i\varphi}V_r(E-\varepsilon_D+e^{i\theta}V_D^2/V_0)]}{e^{2i\theta}V_rV_1^2(e^{6i\varphi}+e^{-2i\varphi})/V_0 + e^{2i\varphi}[(2V_1^2+V_D^2)e^{i\theta} - e^{3i\theta}V_r^2V_D^2/V_0^2 + (E-\varepsilon_D)(V_0-e^{2i\theta}V_r^2/V_0)]}. \tag{12}$$

The behavior of the transmission zero and phase in a three-terminal interferometer as a function of energy for various values of coupling to the third terminal [$V_D=0.1$ (solid), $V_D=0.3$ (dotted), and $V_D=0.6$ (dashed)] is shown in Fig. 2. Unlike a two-terminal closed AB ring with QD's ($V_D=0$),[19,20] it is seen from Fig. 2(a) that in an open ring ($V_D\neq 0$) the Fano resonance peak does not reach unity because of energy loss due to the outgoing electrons into the third terminal. In addition, as V_D increases, the Fano zero [obtained from $N_{21}=0$ in Eq. (4)] shifts progressively further off the real-energy axis into the complex-energy half plane. The Fano zero can be returned to the real energy axis at discrete values of magnetic flux (see below) as long as V_D is less than a critical value. This flexible control over the transmission resonance features is unavailable in a closed, two-terminal interferometer.

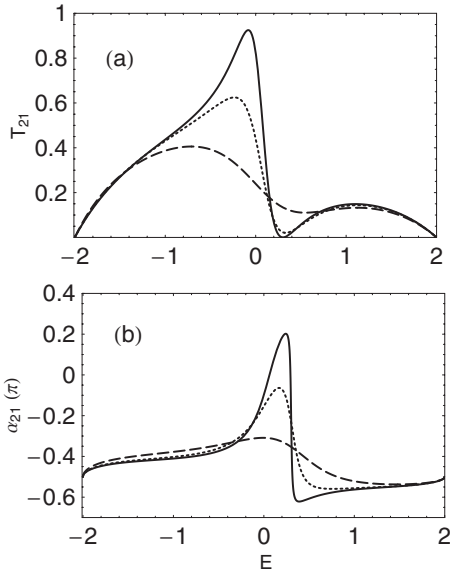

FIG. 2. Transmission T_{21} and transmission phase α_{21} as a function of energy for different values of $V_D=0.1$ (solid curve), $V_D=0.3$ (dotted curve), and $V_D=0.6$ (dashed curve). (a) As V_D increases, the Fano resonance no longer reaches unity and the Fano zero lifts off the real-energy axis. (b) The phase jump of π at the transmission resonance diminishes and softens as the ring is opened with coupling to the third terminal.

In Fig. 2(b), we show the transmission phase as a function of energy for different values of V_D. The transmission phase α_{21}, which can be calculated from Eq. (12) as $\alpha_{21}=\tan^{-1}[\mathrm{Im}(t_{21})/\mathrm{Re}(t_{21})]$, no longer changes abruptly by π at the resonance, as for $V_D=0$, but is shown to progressively soften and to smoothly change by less than π as V_D increases. We attribute this smearing of the abrupt phase jump of π to the fact that current, which flows to the third terminal, breaks unitarity and disrupts the interference effects due to repeated reflections of the electrons from the junctions and back through the ring.

In order to illustrate the transmission phase changing from an abrupt jump to a smooth transition of less than π in a three-terminal AB ring, we calculate the phase using a simple analytical model which is based on the properties of the Fano resonance. In the vicinity of the Fano resonance in the transmission versus electron energy for an AB ring with an embedded QD, the transmission amplitude has the form:[21]

$$t_{21} \cong t_{bg}\left(\frac{E-\tilde{E}_0}{E-E_R+i\Gamma}\right). \tag{13}$$

Here, $\tilde{E}_0$ is the position of the transmission zero and E_R gives the energy of the pole. The width of the resonance Γ indicates how far the pole is off the real-energy axis, and t_{bg} represents any background contribution to the amplitude. Because the Fano transmission zero lies off the real-energy axis for an open ring, we can write $\tilde{E}_0$ in a complex form, $\tilde{E}_0=E_0-i\gamma$. The transmission amplitude can now be written as the product of two complex terms,

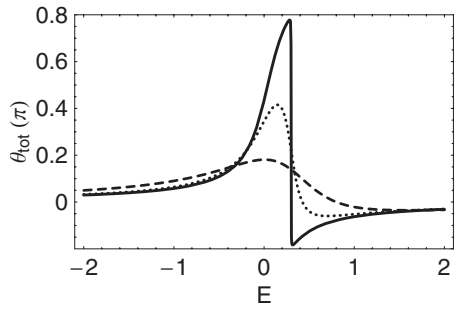

FIG. 3. Modeled transmission phase θ_{tot} vs energy E for a standard Fano resonance (solid curve: E_0=0.3, γ=0.0005, E_R=0.04, Γ=0.192), and for modified Fano resonances (dotted curve: E_0 =0.3, γ=0.1, E_R=0.05, Γ=0.3; dashed curve: E_0=0.38, γ=0.45, E_R=0.1, Γ=0.75) based on the approximate positions of the Fano zeros and poles for V_D=0.01, 0.3, 0.6, respectively. The phase jump of π at the transmission resonance diminishes and softens as V_D increases.

$$t_{21} \cong t_{bg}\frac{(E-E_0+i\gamma)(E-E_R-i\Gamma)}{(E-E_R)^2+\Gamma^2} = |t_{21}|e^{i\theta_{tot}}, \qquad (14)$$

where θ_{tot} is the combined transmission phase from the two complex terms. By separating Eq. (14) into its real and imaginary parts, we obtain an expression for θ_{tot} as

$$\theta_{tot} = \arctan\left[\frac{(E-E_R)\gamma-(E-E_0)\Gamma}{(E-E_R)(E-E_0)+\gamma\Gamma}\right]. \qquad (15)$$

In Eq. (15) for θ_{tot}, there is no sharp phase jump at a particular value of energy, as exists at E=E_R for a two-terminal closed ring in which the Fano zero is on the real-energy axis (γ=0). In Fig. 3, we show plots of θ_{tot} versus E for various coupling parameters V_D to the third terminal. It is clearly seen that as V_D is increased from zero, the abrupt phase jump of π at the resonance softens and diminishes in magnitude. This indicates that the Onsager relations (unitarity and time reversal symmetry) are not valid for an open AB interferometer with an embedded QD.[8,22]

Since the Fano zero and resonance pole in the transmission can be tuned by the magnetic flux Φ threading the AB ring, we investigate the magnetic flux dependence of transmission T_{21} for a fixed V_D. In Fig. 4, the total transmission as a function of electron energy (the left column) and contour plots of the transmission amplitude in the complex-energy plane (the right column) with fixed V_D=0.3 are shown for different magnetic flux values: Φ/Φ_0=0.0, 0.25, 0.548, 0.75, and 0.952 (top to bottom). As the magnetic flux is increased from Φ=0, the Fano zero begins to move on a counterclockwise orbit around the Fano pole. At Φ/Φ_0=0.25, the zero is positioned directly below the Fano pole in the complex-energy plane. As Φ continues to increase, the Fano zero moves back up towards the real-energy axis and crosses the axis at Φ/Φ_0=0.548. When Φ/Φ_0=0.75, the Fano zero arrives directly above the Fano pole, attaining its most positive imaginary value. As the flux is further increased towards Φ/Φ_0=1.0, the Fano zero again *crosses* the real-energy axis at Φ/Φ_0=0.952 on the way back to its position from which it started at Φ/Φ_0=0.

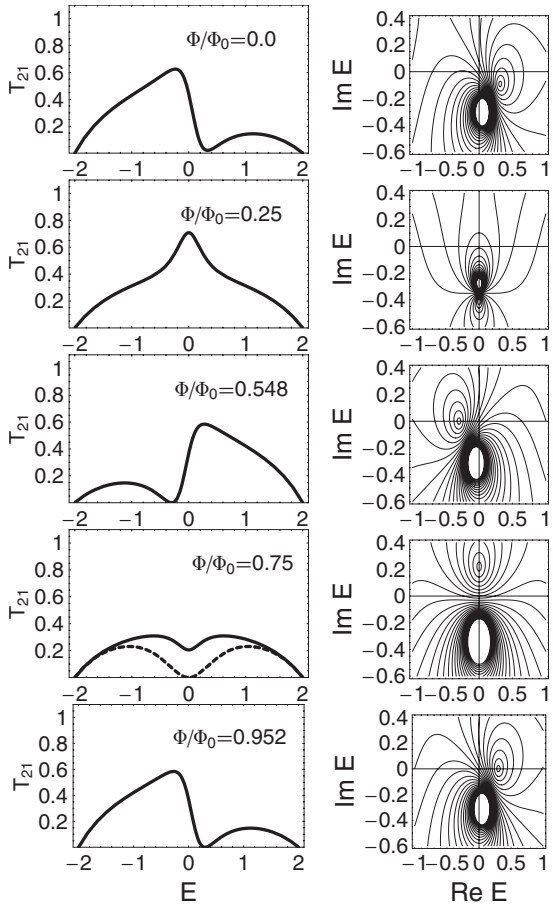

FIG. 4. The total transmission, T_{21}, as a function of electron energy (the left column) and contour plots of the transmission amplitude in the complex-energy plane (the right column) with fixed V_D=0.3, for different magnetic flux Φ/Φ_0=0.0, 0.25, 0.548, 0.75, and 0.952 (top to bottom). The Fano zero moves directly downward and crosses the real-energy axis at V_D=V_D^{crit}, shown in the dashed curve for Φ/Φ_0=0.75.

It is interesting to note from Fig. 4 that for a fixed value of V_D, there exist two values of magnetic flux for which the Fano zero *crosses* the real-energy axis. By setting $V_r[V_0(E-\varepsilon_D)+e^{i\theta}V_D^2]-e^{-4i\varphi}V_0V_1^2$=0 from Eq. (4), the analytical expression for the energy values of the Fano zeros (E_0) and the corresponding normalized magnetic flux values (Φ/Φ_0) in terms of the coupling parameter V_D can be obtained as

$$E_0 = \pm\sqrt{\frac{(V_1^2V_0/V_r)^2-V_D^4}{V_0^2-V_D^2}} \quad \text{and}$$

$$\cos\left[2\pi\left(1-\frac{\Phi}{\Phi_0}\right)\right] = \pm\sqrt{\frac{1-(V_rV_D^2/V_0V_1^2)^2}{1-V_D^4/(2V_0^2-V_D^2)^2}}. \qquad (16)$$

Here, it is required that both the real and imaginary parts of N_{21} from Eq. (4) be zero. For the parameters used in Fig. 4 (V_0=1.0, V_1=V_r=0.3, and V_D=0.3), the two Fano zeros are at E_0=−30 and 0.30 when Φ/Φ_0=0.548 and 0.952, respectively. Notice, however, that there is a critical value of V_D^{crit} [V_D^{crit}=$V_1\sqrt{V_0/V_r}$, obtained from requiring E_0 to be real

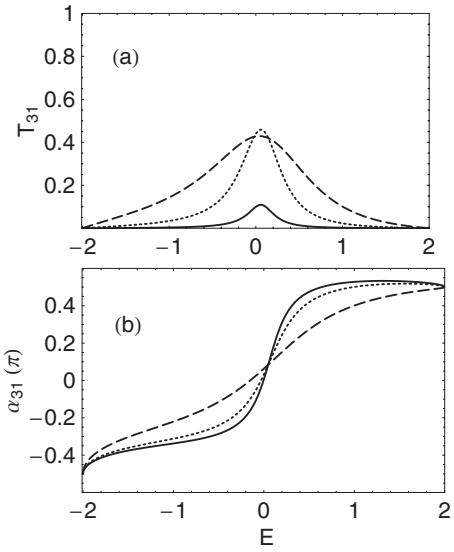

FIG. 5. Transmission T_{31} and transmission phase α_{31} as a function of energy for different values of V_D=0.1 (solid curve), V_D =0.3 (dotted curve), and V_D=0.6 (dashed curve). (a) The BW resonances, which arise from the fact that the amplitude t_{31} does not have zeros in the energy plane, are seen for a variation of V_D. (b) The phase change near the BW resonance softens as V_D increases.

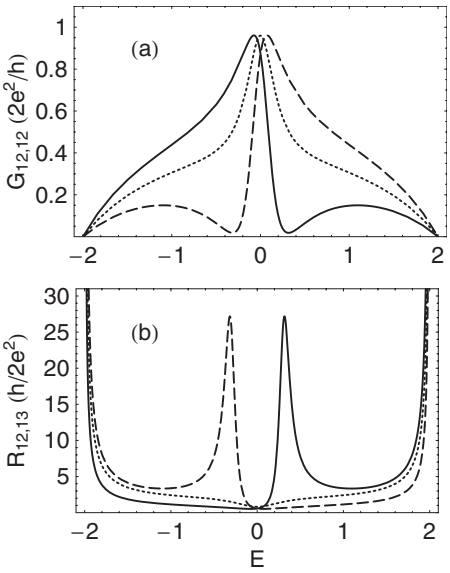

FIG. 6. (a) The conductance $G_{12,12}$ and (b) the resistance $R_{12,13}$ are depicted as a function of electron energy with a fixed V_D=0.1 for different magnetic flux Φ/Φ_0=0.0 (solid curve), 0.25 (dotted curve), and 0.5 (dashed curve). As Φ increases, the swing from Fano to BW resonance (or vice versa) appears in the conductance $G_{12,12}$, and the resistance $R_{12,13}$ increases dramatically near the zero of the Fano resonance.

in Eq. (16)], which is the *maximum* value of V_D for which there is the possibility of placing the Fano zero on the real-energy axis at any value of flux. We show in Fig. 4 that the Fano zero moves directly downward and crosses the real-energy axis at V_D^{crit} [see the dashed transmission curve for Φ/Φ_0=0.75]. When $V_D > V_D^{crit}$, the Fano zero passes into the negative complex-energy half plane and there is no value of flux which can bring the Fano zero back to the real-energy axis.

In contrast to amplitude t_{21}, the cross amplitudes t_{31} and t_{32} do not have zeros in the allowed region of the energy plane [see Eq. (5)] and hence, the behavior of the amplitudes near the pole is expected to be similar to that of the amplitudes near a BW resonance. The transmission T_{31} and the transmission phase α_{31} in the absence of magnetic flux for different coupling parameters, V_D=0.1, 0.3, and 0.6, are shown in Fig. 5 as solid, dotted, and dashed curves, respectively. A simple BW resonance peak in T_{31}, which is less than unity, can clearly be seen in Fig. 5(a) and the corresponding smooth phase change, α_{31}, near the BW resonance is depicted in Fig. 5(b). Notice here that α_{31} at the resonance progressively softens as V_D increases, but the BW peak near $E \approx 0$ has a maximum amplitude at V_D=0.5 for the system parameters used here.

Finally, we investigate the magnetic flux dependence of the conductance $G_{12,12}$ and the resistance $R_{12,13}$ for an open ring with a fixed V_D. In Fig. 6(a), the conductance $G_{12,12}$ as a function of electron energy E with a fixed V_D=0.1 is shown for different values of magnetic flux Φ/Φ_0=0.0 (solid), 0.25 (dotted), and 0.5 (dashed). As Φ increases, a transition from Fano resonance (asymmetry parameter $q<0$, peak$\rightarrow$dip) to BW resonance and then back to Fano resonance ($q>0$, dip $\rightarrow$peak) in $G_{12,12}$ can be observed as a sequence. The Fano resonance produces a very strong influence on the resistance $R_{12,13}$. As shown in Fig. 6(b), the resistance increases dramatically when the electron energy approaches the zero energy E_0 of the Fano resonance. The appearance of the peak in the resistance near the zero of the Fano resonance is connected with almost full reflection of the electron waves traveling from terminal 1 to terminal 2. This indicates that at this Fermi energy there is an additional interference resistance in the circuit region between terminals 1 and 3.

In summary, we have studied the Fano zero and transmission phase for a QD embedded in one arm of a three-terminal AB ring using the exactly solvable tight-binding formalism. A variation of the coupling to the third terminal of the AB ring shifts the zero of the Fano transmission resonance into the complex-energy plane, and softens the abrupt phase jump of π at the resonance. A unique interplay between the magnetic flux threading the ring and coupling to the third terminal opens up a regime of parameter space in which the Fano zero can be returned to the real-energy axis. A manifestation of Fano resonances gives rise to unusual behavior of the conductance (resistance) of a three-terminal ring as a function of Fermi energy in the presence of magnetic field. These results may have applications in further experimental studies of mesoscopic AB interferometers in which phase and resonance properties continue to be of interest.[14,22,23]

One of the authors (E.R.H.) is partially supported by a grant from the Center for Energy Research, Education, and Service at Ball State University. The work of A.M.S. was supported in part by the Russian Basic Research Foundation Grant No. 05-02-16762.

[1] U. Fano, Phys. Rev. **124**, 1866 (1961).
[2] A. Yacoby, M. Heiblum, D. Mahalu, and H. Shtrikman, Phys. Rev. Lett. **74**, 4047 (1995).
[3] R. Schuster, E. Buks, M. Heiblum, D. Mahalu, V. Umansky, and H. Shtrikman, Nature (London) **385**, 417 (1997).
[4] S. Katsumoto, K. Kobayashi, H. Aikawa, A. Sano, and Y. Iye, Superlattices Microstruct. **24**, 151 (2003).
[5] A. Aharony, O. Entin-Wohlman, T. Otsuka, S. Katsumoto, H. Aikawa, and K. Kobayashi, Phys. Rev. B **73**, 195329 (2006).
[6] A. Yacoby, R. Schuster, and M. Heiblum, Phys. Rev. B **53**, 9583 (1996).
[7] L. Onsager, Phys. Rev. **38**, 2265 (1931).
[8] O. Entin-Wohlman, A. Aharony, Y. Imry, Y. Levinson, and A. Schiller, Phys. Rev. Lett. **88**, 166801 (2002).
[9] A. Aharony, O. Entin-Wohlman, B. I. Halperin, and Y. Imry, Phys. Rev. B **66**, 115311 (2002).
[10] A. Aharony, O. Entin-Wohlman, and Y. Imry, Physica E (Amsterdam) **29**, 283 (2005).
[11] M. Sigrist, A. Fuhrer, T. Ihn, K. Ensslin, S. E. Ulloa, W. Wegscheider, and M. Bichler, Phys. Rev. Lett. **93**, 066802 (2004).
[12] A. Yahalom and R. Englman, Phys. Rev. B **74**, 115328 (2006).
[13] T. Kubo, Y. Tokura, T. Hatano, and S. Tarucha, Phys. Rev. B **74**, 205310 (2006).
[14] K. Kobayashi, H. Aikawa, S. Katsumoto, and Y. Iye, Phys. Rev. Lett. **88**, 256806 (2002).
[15] V. Moldoveanu, M. Tolea, V. Gudmundsson, and A. Manolescu, Phys. Rev. B **72**, 085338 (2005).
[16] Y. Aharonov and D. Bohm, Phys. Rev. **115**, 485 (1959).
[17] E. R. Hedin, A. M. Satanin, and Y. S. Joe (unpublished).
[18] M. Büttiker, Phys. Rev. Lett. **57**, 1761 (1986).
[19] Y. S. Joe, A. M. Satanin, and G. Klimeck, Phys. Rev. B **72**, 115310 (2005).
[20] A. M. Satanin, E. R. Hedin, and Y. S. Joe, Phys. Lett. A **349**, 45 (2006).
[21] W. Porod, Z. A. Shao, and C. S. Lent, Phys. Rev. B **48**, 8495 (1993).
[22] A. Aharony, O. Entin-Wohlman, and Y. Imry, Turk. J. Phys. **27**, 1 (2003); Phys. Rev. Lett. **90**, 156802 (2003).
[23] A. Aharony, O. Entin-Wohlman, T. Otsuka, S. Katsumoto, H. Aikawa, and K. Kobayashi, Phys. Rev. B **73**, 195329 (2006).